



Since January 2020 Elsevier has created a COVID-19 resource centre with free information in English and Mandarin on the novel coronavirus COVID-19. The COVID-19 resource centre is hosted on Elsevier Connect, the company's public news and information website.

Elsevier hereby grants permission to make all its COVID-19-related research that is available on the COVID-19 resource centre - including this research content - immediately available in PubMed Central and other publicly funded repositories, such as the WHO COVID database with rights for unrestricted research re-use and analyses in any form or by any means with acknowledgement of the original source. These permissions are granted for free by Elsevier for as long as the COVID-19 resource centre remains active.

HOSTED BY



Contents lists available at ScienceDirect

Saudi Pharmaceutical Journal

journal homepage: www.sciencedirect.com



Original article

## *In vitro* evaluation of nebulized eucalyptol nano-emulsion formulation as a potential COVID-19 treatment

Alaa S. Tulbah<sup>a,\*</sup>, Ammar Bader<sup>b</sup>, Hui Xin Ong<sup>c,d</sup>, Daniela Traini<sup>c,d</sup><sup>a</sup> Department of Pharmaceutics, College of Pharmacy, Umm Al-Qura University, Makkah, Saudi Arabia<sup>b</sup> Department of Pharmacognosy, College of Pharmacy, Umm Al-Qura University, Makkah 21955, Saudi Arabia<sup>c</sup> Respiratory Technology, Woolcock Institute of Medical Research, NSW, Australia<sup>d</sup> Macquarie Medical School, Faculty of Medicine, Health and Human Sciences, Macquarie University, Australia

## ARTICLE INFO

## Article history:

Received 27 June 2022

Accepted 17 September 2022

Available online xxxx

## Keywords:

COVID-19

Eucalyptol

1,8-cineole

Nano-emulsion

Tween 80

Cytotoxicity

## ABSTRACT

Coronavirus is a type of acute atypical respiratory disease representing the leading cause of death worldwide. Eucalyptol (EUC) known also as 1,8-cineole is a potential inhibitor candidate for COVID-19 (main protease-M<sup>Pro</sup>) with effective antiviral properties but undergoes physico-chemical instability and poor water solubility. Nano-emulsion (NE) is a promising drug delivery system to improve the stability and efficacy of drugs. This work focuses on studying the anti- COVID-19 activity of EUC by developing nebulized eucalyptol nano-emulsion (EUC-NE) as a potentially effective treatment for COVID-19. The EUC -NE formulation was prepared using Tween 80 as a surfactant. *In vitro* evaluation of the EUC-NE formulation displayed an entrapment efficiency of 77.49 %, a droplet size of 122.37 nm, and an EUC % release of 84.7 %. The aerodynamic characterization and cytotoxicity of EUC-NE formulation were assessed, and results showed high lung deposition and low inhibitory concentration. The antiviral mechanism of the EUC-NE formulation was performed, and it was found that it exerts its action by virucidal, viral replication, and viral adsorption. Our results confirmed the antiviral activity of the EUC-NE formulation against COVID-19 and the efficacy of nano-emulsion as a delivery system, which can improve the cytotoxicity and inhibitory activity of EUC.

© 2022 The Authors. Published by Elsevier B.V. on behalf of King Saud University. This is an open access article under the CC BY-NC-ND license (<http://creativecommons.org/licenses/by-nc-nd/4.0/>).

## 1. Introduction

COVID-19, an acute respiratory infection caused by the SARS-CoV-2 virus (Jiang et al., 2020; Richardson et al., 2020; Tulbah and Lee, 2021), is currently one of the major cause of death worldwide (Ciotti et al., 2020; Tulbah, 2021). COVID-19 treatment has recently focused on M<sup>Pro</sup> - the enzyme as a target because it is responsible for the Coronavirus replication (Panikar et al., 2021; Sharma, 2020; Sharma and Inderjeet, 2020; Valussi et al., 2021). Eucalyptol (EUC) is the principal component found in *Eucalyptus* sp. essential oils as well as in many aromatic and culinary herbs.

(Abdalla et al., 2020; Monteiro et al., 2021; Panikar et al., 2021; Sharma, 2020; Sharma and Inderjeet, 2020; Valussi et al., 2021). It is a potential inhibitor candidate for COVID-19 M<sup>Pro</sup> (Panikar et al., 2021; Sharma, 2020; Sharma and Inderjeet, 2020; Valussi et al., 2021). EUC also has antiviral, anti-inflammatory, and immunomodulatory properties, and several respiratory diseases such as rhinosinusitis, bronchitis, asthma, and chronic obstructive pulmonary disorder (COPD) (Abdalla et al., 2020; Asif et al., 2020; Yadalam et al., 2021). Recent studies have revealed that EUC may reduce the risk of COVID-19 (Bravo et al., 2021; Panikar et al., 2021; Sharma, 2020; Valussi et al., 2021; Yadalam et al., 2021). However, EUC's bioavailability and efficacy were hindered *in vivo* because it is volatile, instable, and hydrophobic properties (Gamal et al., 2021; Izham et al., 2021; Peng et al., 2021).

Submicron-sized emulsions, known as nano-emulsions, are utilized as drug carriers to enhance the stability and efficacy of therapeutic substances (Fernandez et al., 2004; Shah et al., 2010; Tulbah, 2022). Nano-emulsions are o/w dispersions with droplets size ranging from 100 to 600 nm (Fernandez et al., 2004; Shah et al., 2010). Using a suitable surfactant, these emulsions are created by mixing two immiscible liquids (water and oil) to produce

\* Corresponding author.

E-mail addresses: [astulbah@uqu.edu.sa](mailto:astulbah@uqu.edu.sa) (A.S. Tulbah), [ambader@uqu.edu.sa](mailto:ambader@uqu.edu.sa) (A. Bader), [hong3117@uni.sydney.edu.au](mailto:hong3117@uni.sydney.edu.au) (H.X. Ong), [daniela.traini@mq.edu.au](mailto:daniela.traini@mq.edu.au) (D. Traini).

Peer review under responsibility of King Saud University.



Production and hosting by Elsevier

<https://doi.org/10.1016/j.jsps.2022.09.014>

1319-0164/© 2022 The Authors. Published by Elsevier B.V. on behalf of King Saud University.

This is an open access article under the CC BY-NC-ND license (<http://creativecommons.org/licenses/by-nc-nd/4.0/>).

Please cite this article as: A.S. Tulbah, A. Bader, H.X. Ong et al., *In vitro* evaluation of nebulized eucalyptol nano-emulsion formulation as a potential COVID-19 treatment *In vitro* evaluation of nebulized eucalyptol nano-emulsion formulation →, Saudi Pharmaceutical Journal, <https://doi.org/10.1016/j.jsps.2022.09.014>

a single-phase that is thermodynamically stable (Jaiswal et al., 2015; Solans et al., 2005). Nano-suspensions/ emulsions have been shown to be effective in medication delivery using lipid-insoluble and water medicines. They are enhancing drugs in terms of its integrity, dissolution speed, dependability and saturation solubility (Abd Elkodous et al., 2021). A study by Muthurulappan et al, found that the efficacy of fucoxanthin had been improved and overcome its issue when it was formulated as nano-Suspension (Muthurulappan and Francis, 2013). COVID-19 therapy should be administered through the pulmonary route rather than the oral route because the possible decrease in systemic toxicity, higher local concentration of drugs, and avoidance of first-pass metabolism (Lee et al., 2018; Tulbah and Gamal, 2021; Tulbah et al., 2014), with nebulizers commonly used to deliver aerosolized medications to patients with the respiratory disease (Hess et al., 1996; Khairnar et al., 2022). This work focuses on studying the anti-COVID-19 activity of EUC by developing nebulized eucalyptol nano-emulsion as a promising treatment for COVID-19, as well as studying the physicochemical, aerodynamic characteristics, and in vitro toxicity of eucalyptol nano-emulsion on the Vero-E6 cell line.

## 2. Materials and methods

### 2.1. Materials

Sigma-Aldrich Chemical (MO, USA) supplied chloroform, methanol, eucalyptol, and tween 80. The American Type Culture Collection (Manassas, VA, USA) supplied the Vero-E6 cell lines and cell culture materials.

### 2.2. Quantification of Eucalyptol

The amount of EUC was quantified by a TRACE Ultra gas Chromatograph (THERMO Scientific Corp., USA) equipped with a mass spectrometer detector and a TR-5 MS column (Sa et al., 2021). The temperature was set at 280 °C with a program starting from 100 °C and raised by 4 °C/min. The electron ionization (EI), spectral range, and sample injection were set at 70 eV,  $m/z$  40–450, and 1  $\mu$ l, respectively. At a flow rate of 2.25 ml/min and a split ratio of 1: 5, helium was used as a carrier gas.

### 2.3. Preparation of Eucalyptol Nano-emulsions formulation

The Oil/Water (O/W) Eucalyptol nano-emulsions formulation (EUC-NE) was manufactured following spontaneous emulsification according to a method by Bouchemal, et al. with some modifications (Bouchemal et al., 2004). As shown in Table 1, EUC was added to a mixture of distilled water and Tween 80 and homogenized (Ultra-Turrax T25, Germany) for 25 min at 13000 rpm for 5 cycles. Tween 80 (HLB 15) was used as a surfactant based on a literature review to prepare nano-emulsion with the optimum size, flow, and EE (Bouchemal et al., 2004; Kaplan et al., 2019; López-Montilla et al., 2002). All steps were performed at room temperature and then the formulation was stored at 4 °C before further evaluation. Free eucalyptol liquid was used as a control.

**Table 1**

Design and in vitro evaluation of EUC-NE formulation- Data are presented as Mean  $\pm$  SD.

Formulation	EUC	Tween 80	Water	%EE	Droplet size	Zeta potential	PDI	Release
EUC-NE	4 %v/v	16 %v/v	80 %v/v	77.49 $\pm$ 6.07 %	122.37 $\pm$ 2.66 nm	-13 $\pm$ 1.4 mV	0.36 $\pm$ 0.01	84.7 $\pm$ 4.1 %
EUC	99 % Eucalyptol	0	0		298.06 $\pm$ 14.39 nm	0.02 $\pm$ 0.07 mV	0.42 $\pm$ 0.06	98.17 $\pm$ 2.85 %

### 2.4. Fourier transform infrared spectroscopy (FTIR)

To confirm the presence of EUC within the EUC-NE formulation, a sample of EUC, Tween 80, and EUC-NE formulation was placed inside FTIR (FTIR-8400 s, Shimadzu, Japan) (Herculano et al., 2015). Potassium bromide (100 mg) was added to each sample and the detection was conducted at 4000–500  $\text{cm}^{-1}$ .

### 2.5. In vitro evaluation of EUC-NE formulation

#### 2.5.1. Measurement of % entrapment efficiency

To assess the EUC content, the EUC-NE formulation sample was centrifuged (SIGMA, Steinheim, Germany) for 1 h at 20,000 rpm (Abo El-Ela et al., 2020). The supernatant solution was collected and the %EE was calculated in triplicates using the GC-MS method as follows:

$$\%EE = (B - A)/B \times 100 \quad (1)$$

where A is the drug amount in supernatant and B is the total drug amount.

#### 2.5.2. Evaluation of zeta potential and droplet size

Droplet size, polydispersity index (PDI), and zeta potential of EUC-NE formulation were assessed using Dynamic Light Scattering (DLS, Zetasizer, Malvern, UK) (Tulbah and Gamal, 2021). At 25 °C, samples were tested after being diluted in ultra-purified water.

#### 2.5.3. In vitro release studies

To ensure the sink conditions to assess EUC's release, the solubility, and dissolution volume of EUC were assessed by stirring excess amount of EUC in phosphate buffer saline (PBS, pH 7.4) for 3 days at 25 °C and the amount dissolved was measured using the GC-MS method in triplicate. The studied samples were free EUC, and EUC-NE formulations, and the diffusion membrane was a dialysis bag (Tulbah et al., 2017). At 100 rpm, the studied samples were rotated and at each time interval, the amount of EUC dissolved was measured using the GC-MS method in triplicate.

#### 2.5.4. Kinetic analysis of release data

To assess the model that fits the EUC-NE formulation's release, coefficient of determination ( $R^2$ ), Akaike information criterion (AIC), and model selection criterion (MSC) criteria were assessed using DDSolver software (Salem et al., 2022). The Korsmeyer-Peppas equation and similarity factor " $f_2$ " were used to assess the release mechanism and the significant ( $p < 0.05$ ) difference between EUC-NE and free EUC dissolution profiles, respectively.

### 2.6. Transmission electron microscopy (TEM) measurement

Transmission Electron Microscopy (TEM, JEOL, Japan) was used to assess the morphology of the EUC-NE formulation at suitable magnifications (Tulbah et al., 2019). Before observations, the EUC-NE formulation was put onto a carbon-coated copper grid and air-dried.

## 2.7. Aerodynamic characterization

To assess the aerodynamic characterization of the EUC-NE formulation, a sample was jet nebulized (VixOne, AZ, USA) through a cooled (4 °C) Andersen MKII cascade impactor (ACI, Copley Scientific, UK) at a flow rate of (15 l/min (Abdelrahim, 2011; Tulbah et al., 2015), using a calibrated flow meter (ADD MAKE). Each part of the ACI was washed with a 20 % v/v methanol and the EUC's amount was calculated in triplicates using the GC-MS method. Copley Inhaler Testing Data Analysis Software (Copley Scientific, UK) was used to determine the fine particle dose (FPD) which is the dose of the aerosolized drug with an aerodynamic diameter, fine particle fraction (FPF) which is the dose fraction < 5 µm and deposited in the lung, and the mass median aerodynamic diameter (MMAD).

## 2.8. In vitro bio-characterization of EUC-NE formulation

### 2.8.1. Cell culture

Vero E6 cell line was selected because they express the SARS-CoV-2 S protein for SARS-CoV replication (Ogando et al., 2020; Wurtz et al., 2021). Cell culture materials consisting of DMEM medium (1 % of penicillin/streptomycin and 10 % of FBS) were used to preserve Vero-E6 cells which then were distributed in each well of 96-well cells (100 µl/well at a density of  $3 \times 10^5$  cells/ml) culture plates and incubated overnight at 37 °C with 5 % CO<sub>2</sub> (Mostafa et al., 2020). The cells were added into a T-175 flask for up to 24 h to make a virus stock and then isolated in the infection medium consisting of 1 % L-1-tosylamido-2-phenylethyl chloromethyl ketone (TPCK)-treated trypsin, and a DMEM medium with 2 % FBS. The infection was occurred by swapping hCoV-19/Egypt/NRC-3/2020 virus (Accession Number on GSAID: EPI\_ISL\_430820) and incubated for up to 3 days with new infection media.

### 2.8.2. Cytotoxicity assay of EUC-NE on Vero E6 cells

MTT assay was used to evaluate the half-maximal cytotoxic concentration (CC50) of EUC-NE formulation compared to the control cells (untreated) (Mostafa et al., 2020). Vero-E6 cells ( $3 \times 10^5$  cells) were prepared as described before and different concentrations of EUC-NE (7.81–1000 µg/ml) were added. The cells were then incubated with 20 µl of MTT solution, followed by medium aspiration. Each well was filled with an acidified mixture of isopropanol and formazan crystals. %cytotoxicity was determined using the Formazan solution absorbance in triplicates as follows:

$$\% \text{ cytotoxicity} = ((NT - T) / (NT)) \times 100$$

where non-treated cells absorbance (NT) and treated cells absorbance (T).

### 2.8.3. Inhibitory concentration 50 (IC50) determination

The concentration (IC50) of EUC-NE formulation necessary to decrease half of the SARS-CoV-2 virus-induced cytopathic effect compared to the control cells (untreated) was measured (Mostafa et al., 2020; Tulbah and Lee, 2021). Vero-E6 cells ( $2.4 \times 10^4$  cells) were prepared as described above and different concentrations of EUC-NE (7.81–125 µg/ml) were added and incubated for 72 h. The cells were then fixed with 100 µl of paraformaldehyde solution. A mixture of methanol and crystal violet dye was added to each well. IC50 was determined by measuring the colour and its spectral density at 570 nm using a plate reader (Anthos Zenyth 200rt, Anthos Labtec Instruments, Netherlands) in triplicates.

### 2.8.4. Mechanism of action of EUC-NE activity

The plaque infectivity reduction test was used to investigate the mechanism of EUC-NE's antiviral activity (Kuo et al., 2002; Zhang et al., 1995). Untreated Vero-E6 cells directly infected with NRC-03-nhCoV were used as control wells.

### 2.8.5. Mechanism of viral adsorption

Viral adsorption was performed similarly to the method by Zhang et al. (Zhang et al., 1995). The EUC-NE was incubated to the Vero-E6 cells ( $10^5$  cells/ml) at 4 °C for 2 h after they had been cultured in a 6-well plate at 37 °C for 24 h. Diluted SARS-CoV-2 virus ( $10^4$  PFU/well) and DMEM (3 ml, 2 % agarose) were added and co-incubated for 1 h. Viral plaques formed when plates were allowed to harden and then hatched at 37 °C. To calculate the %reduction in plaque formation of EUC-NE compared to that of control wells, the plaques were stained with crystal violet after being fixed in a 10 % formalin solution for 1 h.

### 2.8.6. Viral replication mechanism

Viral replication was tested as described by Kuo et al. (Kuo et al., 2002). The SARS-CoV-2 virus was incubated to the Vero-E6 cells ( $10^5$  cells/ml) for 1 h after they had been cultured in a 6-well plate at 37 °C for 24 h. EUC-NE and DMEM (3 ml, 2 % agarose) were added and co-incubated for 1 h. Viral plaques formed when plates were allowed to harden and then hatched at 37 °C. To calculate the %reduction in plaque formation of EUC-NE compared to that of control wells, the plaques were coloured with crystal violet after being fixed in a 10 % formalin solution for 1 h.

### 2.8.7. Virucidal mechanism

Virucidal mechanisms were assayed as described by Zhang et al. (Zhang et al., 1995). The SARS-CoV-2 virus was incubated with EUC-NE and diluted using serum-free DMEM to allow viral growth on Vero-E6 cells when incubated. Viral plaques formed when plates were allowed to harden and then hatched at 37 °C. To calculate the %reduction in plaque formation of EUC-NE compared to that of control wells, after being fixed in a 10 % formalin solution for 1 h, the plaques were colored with crystal violet.

## 2.9. Statistical analysis

Each testing was conducted in triplicate and data are expressed as mean ± standard deviation (SD). Analysis of data is done using a Student T-test. A p-value of < 0.05 is considered statistically significant. IBM-SPSS Statistics (version 22, USA, p 0.05) was utilized.

## 3. Results

### 3.1. Gas Chromatography-mass spectrometry (GC-MS) quantification of eucalyptol

The peak shape for EUC was symmetrical with a retention time of 6.17 min. The constructed calibration curve for EUC was linear over a concentration range of 10–100 ppb with a coefficient of determination (R<sup>2</sup>) of 0.999.

### 3.2. Fourier transform infrared spectroscopy (FTIR)

As shown in Fig. 1, peaks of the EUC -NE formulation were compared with those of EUC and Tween 80 to explore any peak shifts. The FTIR findings of the EUC-NE formulation show similar peaks to those of EUC and Tween 80, demonstrating the presence of EUC after drug loading.

### 3.3. In vitro evaluation of EUC -NE formulation

Successfully, EUC-NE formulation including EUC (4 %v/v), Tween 80 (16 %v/v), and water (80 %v/v) was prepared using spontaneous emulsification by Bouchemal, et al. As demonstrated in Table 1, droplet size, %EE, polydispersity index (PDI) and zeta potential of the EUC-NE formulation were measured. The results

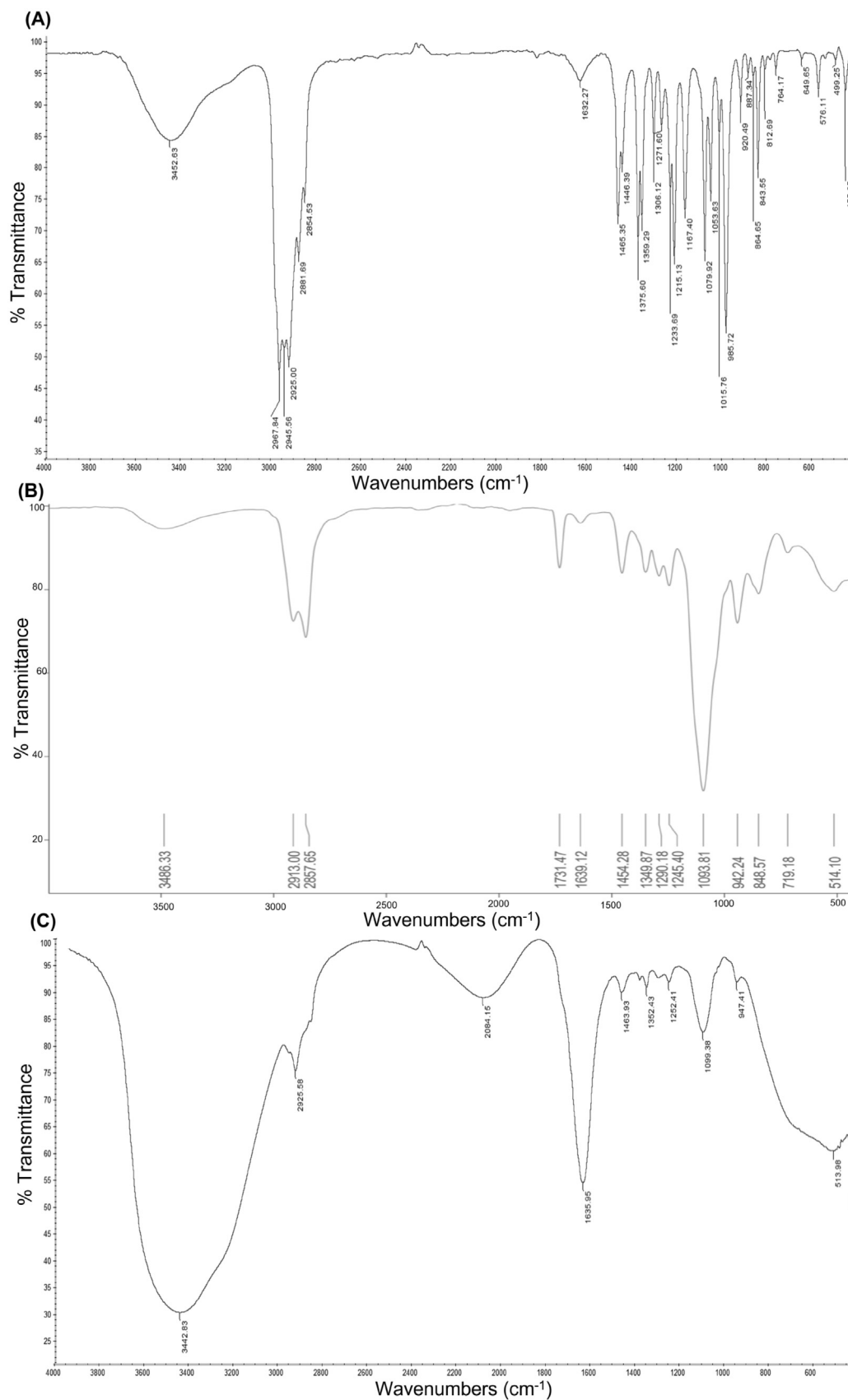


**Fig. 1.** FTIR spectra of EUC -NE formulation components, A), EUC (B), Tween 80 (C), and EUC-NE formulation.

showed that the EUC-NE formulation had a small droplet size and low PDI values. The values of the zeta potential of the EUC-NE formulation indicated a negative surface charge appropriate for electrostatic stabilization. To fulfill the sink condition of the release experiment, the dissolution volume of 25 mM of phosphate buffer saline (PBS, pH 7.4) was used to exceed the saturation solubility of EUC (0.25 mg/ml). As demonstrated in Table 1, the release of free EUC and EUC-NE formulation was measured. Fig. 2 shows that the release of EUC from the EUC-NE formulation was significantly lower than that of free EUC for the 8 h of the experiment. The in vitro release kinetics and mechanism of EUC from the EUC-NE formulation was evaluated using DDSolver software. As shown in Table 2, EUC was released from the EUC-NE formulation by the Higuchi model, which had minimum AIC and maximum R<sup>2</sup> and MSC, and by non Fickian diffusion, which had an estimated “n” of 0.508 ± 0.01. Additionally, the EUC-NE formulation had a significant ( $p < 0.05$ ) different dissolution profile compared to free EUC ( $f_2 = 38.99 \pm 1.96$ ).

#### 3.4. Transmission electron Microscopy (TEM) measurement

Fig. 3 displays the EUC-NE formulation's surface morphology obtained by TEM. Microscopic observation showed the presence of spherical drops.

#### 3.5. Aerodynamic characterization

The aerodynamic deposition of the nebulized EUC-NE formulation was measured using the cascade impactor. Fig. 4 shows the deposition of nebulized EUC-NE formulation on ACI stages. The nebulized EUC-NE formulation has an FPD of 19.11 ± 13.1 mg and an FPF of 56.01 ± 1.7 %, indicating a high drug deposition in the lung. Additionally, the EUC-NE formulation showed a low MMAD of 2.6 ± 0.4 μm indicating suitability for the nebulized EUC-NE formulation to be delivered to the lung.

#### 3.6. In vitro bio-characterization of EUC-NE formulation

##### 3.6.1. Cytotoxicity assay and inhibitory concentration 50 (IC<sub>50</sub>) determination

The cytotoxicity and cell survival of the EUC-NE formulation were investigated using the MTT test to determine the optimal concentration for EUC delivery to the lungs. As shown in Fig. 5,

**Table 2**  
DDSolver release data kinetic models of EUC-NE formulation.

Model	Coefficient of determination	Model Selection Criterion	Akaike Information Criterion
Zero-order	0.8012	1.0717	65.0568
First-order	0.9794	2.0170	56.5496
<b>Higuchi</b>	<b>0.9924</b>	<b>3.532</b>	<b>42.9084</b>
Korsmeyer-Peppas	0.9841	3.3775	44.3052
Hixson-Crowell	0.9024	1.7833	58.6526

the EUC-NE formulation had a CC<sub>50</sub> and an IC<sub>50</sub> of 24.23 μg/ml and 15.939 μg/mL, respectively.

##### 3.6.2. Mechanism of action of EUC-NE activity

Using the plaque infectivity reduction assay, the mechanism of the EUC-NE formulation activity was examined. As shown in Table 3, the EUC-NE formulation exerts its antiviral activity against SARS-CoV-2 by targeting the virus outside the cells (Virucidal), inhibiting viral replication and adsorption.

## 4. Discussion

Eucalyptol is a natural oily monoterpene that has limited water miscibility and low bioavailability, and so it can be incorporated into O/W nano-emulsions to enhance its anti- COVID-19 activity. Consequently, the EUC nano-emulsion formulation was prepared to stabilize EUC and disperse it within an aqueous medium. The structure and concentration of surfactant and physicochemical characteristics of drugs affect the nano-emulsions droplet size and distribution (Bouchemal et al., 2004; Kaplan et al., 2019). The presence of small droplets decreases the mean droplet size and increases droplet surface area enhancing the nano-emulsions characters (Bouchemal et al., 2004; López-Montilla et al., 2002). Increasing the surfactant's HLB value reduces mean droplet size (Bouchemal et al., 2004). Tween 80 (HLB 15) was used as a surfactant based on a literature review to prepare nano-emulsion with the optimum size, flow, and EE (Bouchemal et al., 2004; Kaplan et al., 2019; Seijo et al., 1990). The formulation of the EUC into the NE was confirmed with FTIR studies. To assess the compatibility of nanoparticles' components and any chemical interactions

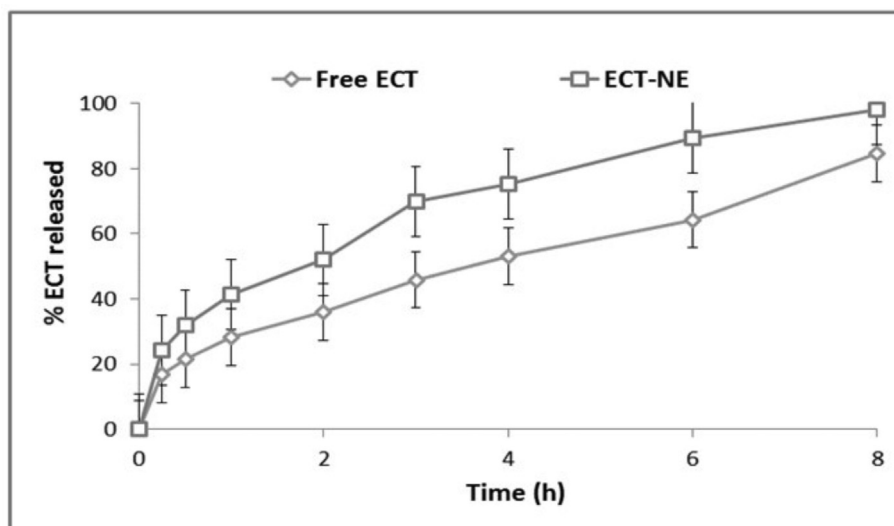


**Fig. 2.** In vitro release profile of EUC-NE formulations ( $n = 3 \pm SD$ ).

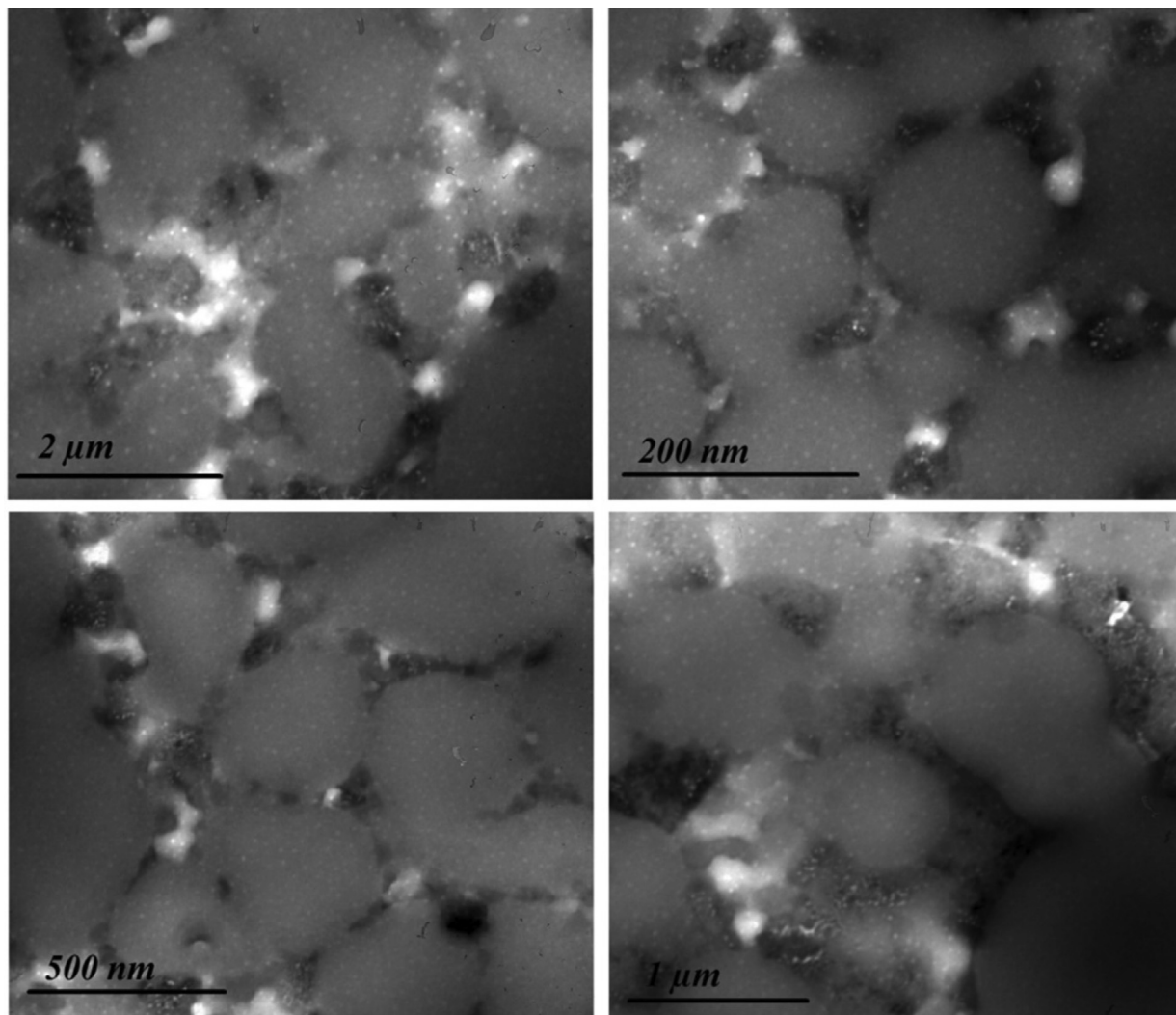


Fig. 3. TEM micrographs of EUC-NE.

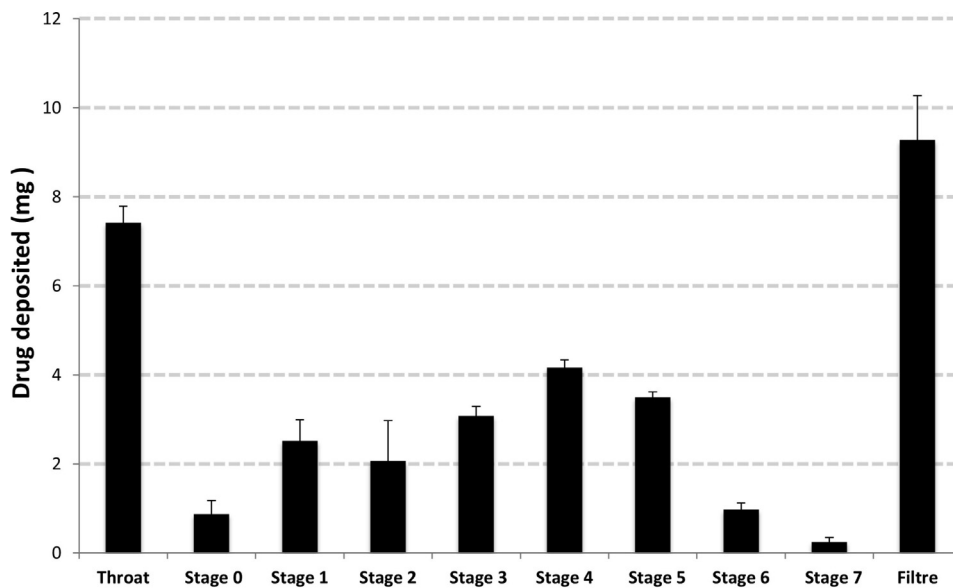


Fig. 4. *In vitro* drug deposition of the nebulized EUC-NE formulation shows a deposited amount of EUC at each ACI stage ( $n = 3 \pm S.D.$ ).

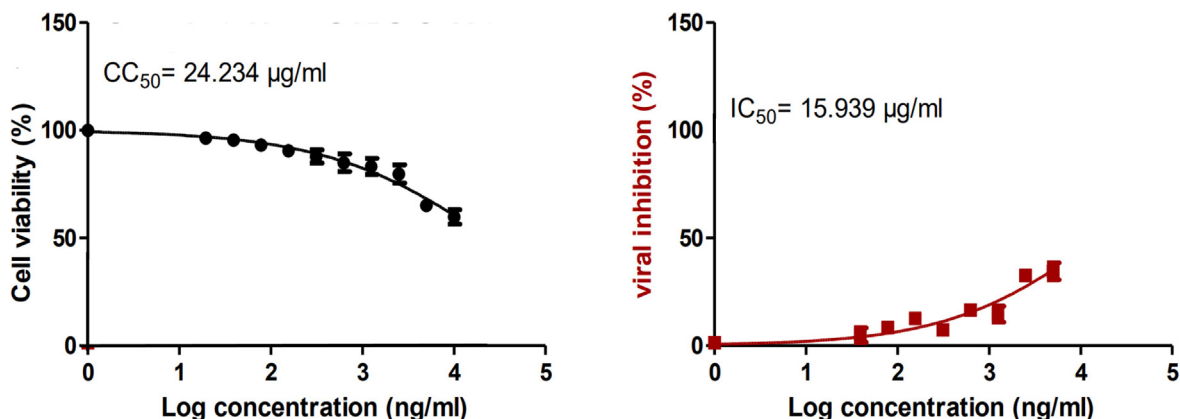


Fig. 5. Left- The cytotoxicity concentration 50 ( $CC_{50}$ ) and Right- viral inhibitory concentration 50 ( $IC_{50}$ ) of EUC-NE formulation on Vero-E6 cells line model.

**Table 3**  
Mechanism of action of EUC -NE.

Code of Sample	Concentration $\mu\text{g/ml}$	Virus Control (PFU/ml)	Viral Titer (PFU/ml)	Viral Inhibition (%)
Virucidal Effect	10	$0.87 \times 10^5$	$0.39 \times 10^5$	55.2 %
	5		$0.42 \times 10^5$	51.7 %
	2.5		$0.57 \times 10^5$	34.5 %
	1.25		$0.63 \times 10^5$	27.6 %
Replication inhibition	10	$0.87 \times 10^5$	$0.29 \times 10^5$	66.7 %
	5		$0.3 \times 10^5$	65.5 %
	2.5		$0.3 \times 10^5$	65.5 %
	1.25		$0.35 \times 10^5$	59.8 %
Adsorption inhibition	10	$0.87 \times 10^5$	$0.29 \times 10^5$	66.7 %
	5		$0.40 \times 10^5$	54 %
	2.5		$0.55 \times 10^5$	36.8 %
	1.25		$0.8 \times 10^5$	8 %

between the components of NE, the FTIR analysis was carried out (Tulbah and Gamal, 2021). There were broad peaks at  $2925 \text{ cm}^{-1}$  in the EUC FT-IR spectrum, indicating alkenes-induced C—H stretching and at  $1465 \text{ cm}^{-1}$  indicating alkane-induced C—H bending. Esters and alcohols produced peaks at  $1215 \text{ cm}^{-1}$  and  $1079 \text{ cm}^{-1}$ . One common peak near  $1635 \text{ cm}^{-1}$  due to C—H bending for alkane groups was detected in pure EUC and EUC-NE formulations. The FTIR findings of the EUC-NE formulation show similar pikes as those of EUC and Tween 80 demonstrating compatibility in the formulation and that EUC is present inside the nanoparticles. FTIR spectra illustrated that EUC was encapsulated in nano-emulsions droplets.

The GC-MS method was used to quantify EUC. Linearity, sensitivity, precision, and accuracy of this method were high (Sa et al., 2021). The prepared formulation's drug content was calculated using the percent EE. When Tween 80 is used as a carrier in nano-emulsion formulations, the efficiency of encapsulation is greatly improved (Song et al., 2011). Tween 80 is a non-ionic surfactant that has a higher HLB value and helps to increase the solubility of EUC (Chaudhari and Kuchekar, 2018; Chuacharoen et al., 2019). Increasing the solubility of the EUC resulted in increased drug loading and better entrapment efficiency of EUC. The results of particle size determination revealed that EUC nano-emulsion was prepared with a small droplet size and narrow PDI demonstrated a homogeneous droplet size distribution. Tween 80 reduced the surface tension of oil drops, which helped the breakdown of the oil drops into smaller sizes (Chaudhari and Kuchekar, 2018). It also allows the effective transport of active ingredients to the lungs. These results were confirmed by microscopic TEM observations, which showed the presence of small spherical drops. Additionally, EUC nano-emulsion was prepared with a negative zeta potential, indicating the potential stability

of the colloidal system due to the presence of electrostatic repulsion between particles (Chaudhari and Kuchekar, 2018; Rodrigues et al., 2018). Enough surfactant was present to cover the oil droplets' surface which stabilized and prevented the coalescence of nano-emulsion droplets (Chaudhari and Kuchekar, 2018). These findings are supported by Chaudhari et al. study (Chaudhari and Kuchekar, 2018). *In vitro* release studies of EUC-NE formulation showed high drug release because the presence of small droplets decreases the mean droplet size and increases droplet surface area (Kaplan et al., 2019) (Chaudhari and Kuchekar, 2018).

The aerodynamic deposition of the nebulized EUC-NE formulation was measured using the cascade impactor. Aerosol particles were characterized by MMAD (Arbain et al., 2018) and results showed suitability for the nebulized EUC-NE formulation to be delivered to the lung. Additionally, the nebulized EUC-NE formulation showed high FPF indicating a high drug deposition. To assess the effect of the EUC -NE formulation on the cytotoxicity and cell viability *in vitro*, the MTT assay was performed. Cell viability results showed a cytotoxic effect of the EUC-NE formulation with a low  $IC_{50}$  value. Antiviral mechanisms of action of the EUC-NE formulation were studied using a plaque infectivity reduction test. By testing the EUC-NE formulation, we found that it exerts its antiviral activity against SARS-CoV-2 by a synergistic effect between virucidal, viral replication, and viral adsorption. As shown in Table 3, the EUC-NE formulation showed a decrease in the viral titer, displaying good antiviral activity compared with the control.

## 5. Conclusion

Eucalyptol is a potential inhibitor candidate for COVID-19  $M^{PFO}$  with effective antiviral properties but undergoes instability and poor water solubility. The EUC nano-emulsion formulation was

prepared to improve the delivery and efficacy of drugs for COVID-19 treatment. The EUC nano-emulsion formulation was nebulized before being characterized to investigate the aerodynamic deposition and antiviral activity of EUC. Our results demonstrated a higher deposition of EUC in the lung, antiviral activity of EUC-NE formulation against SARS-CoV-2, and the efficacy of nano-emulsion as a delivery system, which can improve the cytotoxicity and inhibitory activity of EUC.

### Declaration of Competing Interest

The authors declare that they have no known competing financial interests or personal relationships that could have appeared to influence the work reported in this paper.

### Acknowledgments

Daniela Traini is funded by a Fellowship Grant from the National Health and Medical Research Council (NHMRC) of Australia (APP1173363).

### Funding

Tulbah would like to thank Kingdom of Saudi Arabia - Ministry of Health for funding this project with Grant number: 20 - # 655E (COVID-19 Granted Researched) at 20-04-2020.

### References

- Abd Elkodous, M., Olojede, S., Morsi, M., El-Sayyad, G.S., 2021. Nanomaterial-based drug delivery systems as promising carriers for patients with COVID-19. *RSC Adv.* 11 (43), 26463–26480.
- Abdalla, A.N., Shaheen, U., Abdallah, Q.M.A., Flamini, G., Bkhaitan, M.M., Abdelhady, M.I.S., Ascricchi, R., Bader, A., 2020. Proapoptotic activity of Achillea membranacea essential oil and its major constituent 1, 8-cineole against A2780 ovarian cancer cells. *Molecules* 25 (7), 1582.
- Abdelrahim, M.E., 2011. Aerodynamic characteristics of nebulized terbutaline sulphate using the Andersen Cascade Impactor compared to the Next Generation Impactor. *Pharm. Dev. Technol.* 16 (2), 137–145.
- Abo El-Ela, F.I., Hussein, K.H., El-Banna, H.A., Gamal, A., Roubay, S., Menshaway, A., Salem, H.F., 2020. Treatment of Brucellosis in Guinea Pigs via a Combination of Engineered Novel pH-Responsive Curcumin Niosome Hydrogel and Doxycycline-Loaded Chitosan-Sodium Alginate Nanoparticles: An In Vitro and In Vivo Study. *AAPS PharmSciTech* 21 (8), 1–11.
- Arbain, N., Basri, M., Salim, N., Wui, W., Rahman, M.A., 2018. Development and characterization of aerosol nanoemulsion system encapsulating low water soluble quercetin for lung cancer treatment. *Mater. Today: Proc.* 5, S137–S142.
- Asif, M., Saleem, M., Saadullah, M., Yaseen, H.S., Al Zarzour, R., 2020. COVID-19 and therapy with essential oils having antiviral, anti-inflammatory, and immunomodulatory properties. *Inflammopharmacology* 28 (5), 1153–1161.
- Bouchemal, K., Briançon, S., Perrier, E., Fessi, H., 2004. Nano-emulsion formulation using spontaneous emulsification: solvent, oil and surfactant optimisation. *Int. J. Pharm.* 280 (1–2), 241–251.
- Bravo, J.A., Vila, J.L., Bonté, F., 2021. Eucalyptol and alpha-pinene, natural products with antiviral activity. Personal anti covid-19 prevention method based on essential oils; nasal, oral and manual aqueous cleaning [3xal]. *Coronavirus: environmental disinfection by Eucalyptus. Revista Boliviana de Química* 38 (2), 95–103.
- Chaudhari, P.M., Kuchekar, M.A., 2018. Development and evaluation of nanoemulsion as a carrier for topical delivery system by box-behnken design. *Asian J. Pharm. Clin. Res.* 11, 286–293.
- Chuachroen, T., Prasongsuk, S., Sabliov, C.M., 2019. Effect of surfactant concentrations on physicochemical properties and functionality of curcumin nanoemulsions under conditions relevant to commercial utilization. *Molecules* 24 (15), 2744.
- Ciotti, M., Ciccozzi, M., Terrinoni, A., Jiang, W.-C., Wang, C.-B., Bernardini, S., 2020. The COVID-19 pandemic. *Crit. Rev. Clin. Lab. Sci.* 57 (6), 365–388.
- Fernandez, P., André, V., Rieger, J., Kühnle, A., 2004. Nano-emulsion formation by emulsion phase inversion. *Colloids Surf., A* 251 (1–3), 53–58.
- Gamal, A., Saeed, H., El-Ela, F.I.A., Salem, H.F., 2021. Improving the antitumor activity and bioavailability of sonidegib for the treatment of skin cancer. *Pharmaceutics* 13 (10), 1560.
- Herculano, E.D., de Paula, H.C., de Figueiredo, E.A., Dias, F.G., Pereira, V.D.A., 2015. Physicochemical and antimicrobial properties of nanoencapsulated Eucalyptus staigeriana essential oil. *LWT-Food Sci. Technol.* 61 (2), 484–491.
- Hess, D., Fisher, D., Williams, P., Pooler, S., Kacmarek, R.M., 1996. Medication nebulizer performance: effects of diluent volume, nebulizer flow, and nebulizer brand. *Chest* 110 (2), 498–505.
- Izham, M.N.M., Hussin, Y., Rahim, N.F.C., Aziz, M.N.M., Yeap, S.K., Rahman, H.S., Masarudin, M.J., Mohamad, N.E., Abdullah, R., Alitheen, N.B., 2021. Physicochemical characterization, cytotoxic effect and toxicity evaluation of nanostructured lipid carrier loaded with eucalyptol. *BMC Complement. Med. Therapies* 21 (1).
- Jaiswal, M., Dudhe, R., Sharma, P., 2015. Nanoemulsion: an advanced mode of drug delivery system. *3 Biotech* 5 (2), 123–127.
- Jiang, F., Deng, L., Zhang, L., Cai, Y., Cheung, C.W., Xia, Z., 2020. Review of the clinical characteristics of coronavirus disease 2019 (COVID-19). *J. Gen. Intern. Med.* 35 (5), 1545–1549.
- Kaplan, A.B.U., Cetin, M., Orgul, D., Taghizadehghalehjoughi, A., Hacimuftuoglu, A., Hekimoglu, S., 2019. Formulation and in vitro evaluation of topical nanoemulsion and nanoemulsion-based gels containing daidzein. *J. Drug Delivery Sci. Technol.* 52, 189–203.
- Khairnar, S.V., Jain, D.D., Tambe, S.M., Chavan, Y.R., Amin, P.D., 2022. Nebulizer systems: a new frontier for therapeutics and targeted delivery. *Therapeutic Delivery* 13 (1), 31–49.
- Kuo, Y.-C., Lin, L.-C., Tsai, W.-J., Chou, C.-J., Kung, S.-H., Ho, Y.-H., 2002. Samarangenin B from *Limonium sinense* suppresses herpes simplex virus type 1 replication in Vero cells by regulation of viral macromolecular synthesis. *Antimicrob. Agents Chemother.* 46 (9), 2854–2864.
- Lee, W.-H., Loo, C.-Y., Ghadiri, M., Leong, C.-R., Young, P.M., Traini, D., 2018. The potential to treat lung cancer via inhalation of repurposed drugs. *Adv. Drug Deliv. Rev.* 133, 107–130.
- López-Montilla, J.C., Herrera-Morales, P.E., Pandey, S., Shah, D.O., 2002. Spontaneous emulsification: Mechanisms, physicochemical aspects, modeling, and applications. *J. Dispersion Sci. Technol.* 23 (1–3), 219–268.
- Monteiro, A.C.M., Drame, A.D., Nascimento, F.M., Miranda-Vilela, A.L., Lima, A.V., da Silva, M.A.N., Ribeiro, I.F., 2021. In vitro Inhibitory Action of the Essential Oils of *Origanum Vulgare* and *Rosmarinus Officinalis* against *Aspergillus Fumigatus*. *PlantaMedica Int. Open* 8 (03), e143–e152.
- Mostafa, A., Kandeil, A., AMM Elshaiar, Y., Kutkat, O., Moatasim, Y., Rashad, A.A., Shehata, M., Gomaa, M.R., Mahrous, N., Mahmoud, S.H., GabAllah, M., Abbas, H., Taweel, A.E., Kayed, A.E., Kamel, M.N., Sayes, M.E., Mahmoud, D.B., El-Shesheny, R., Kayali, G., Ali, M.A., 2020. FDA-approved drugs with potent in vitro antiviral activity against severe acute respiratory syndrome coronavirus 2. *Pharmaceutics* 13 (12), 443.
- Muthurilappan, S., Francis, S.P., 2013. Anti-cancer mechanism and possibility of nano-suspension formulation for a marine algae product fucoxanthin. *Asian Pac. J. Cancer Prev.* 14 (4), 2213–2216.
- Ogando, N.S., Dalebout, T.J., Zevenhoven-Dobbe, J.C., Limpens, R.W.A.L., van der Meer, Y., Caly, L., Druce, J., de Vries, J.J.C., Kikkert, M., Bárcena, M., Sidorov, I., Snijder, E.J., 2020. SARS-coronavirus-2 replication in Vero E6 cells: replication kinetics, rapid adaptation and cytopathology. *J. General Virol.* 101 (9), 925–940.
- Panikar, S., Shoba, G., Arun, M., Sahayarayan, J.J., Usha Raja Nanthini, A., Chinnathambi, A., Alharbi, S.A., Nasif, O., Kim, H.-J., 2021. Essential oils as an effective alternative for the treatment of COVID-19: Molecular interaction analysis of protease (Mpro) with pharmacokinetics and toxicological properties. *J. Infect. Public Health* 14 (5), 601–610.
- Peng, J., Jiang, Z., Wu, G., Cai, Z., Du, Q., Tao, L., Zhang, Y., Chen, Y.i., Shen, X., 2021. Improving protection effects of eucalyptol via carboxymethyl chitosan-coated lipid nanoparticles on hyperglycaemia-induced vascular endothelial injury in rats. *J. Drug Target.* 29 (5), 520–530.
- Richardson, P., Griffin, I., Tucker, C., Smith, D., Oechsle, O., Phelan, A., Rawling, M., Savory, E., Stebbing, J., 2020. Baricitinib as potential treatment for 2019-nCoV acute respiratory disease. *Lancet (London, England)* 395 (10223).
- Rodrigues, F., Diniz, L., Sousa, R., Honorato, T., Simão, D., Araújo, C., Gonçalves, T., Rolim, L., Goto, P., Tedesco, A., Siqueira-Moura, M., 2018. Preparation and characterization of nanoemulsion containing a natural naphthoquinone. *Química Nova*.
- Sa, C., Liu, J., Dong, Y., Jiang, L., Gentana, G., Wurita, A., 2021. Quantification of eucalyptol (1, 8-cineole) in rat serum by gas chromatography-mass/mass spectrometry and its application to a rat pharmacokinetic study. *Biomed. Chromatogr.* 35 (6), e5080.
- Salem, H.F., Gamal, A., Saeed, H., Kamal, M., Tulbah, A.S., 2022. Enhancing the Bioavailability and Efficacy of Vismodegib for the Control of Skin Cancer: In Vitro and In Vivo Studies. *Pharmaceutics* 15 (2), 126.
- Seijo, B., Fattal, E., Roblot-Treupel, L., Couvreur, P., 1990. Design of nanoparticles of less than 50 nm diameter: preparation, characterization and drug loading. *Int. J. Pharm.* 62 (1), 1–7.
- Shah, P., Bhalodia, D., Shelat, P., 2010. Nanoemulsion: A pharmaceutical review. *System. Rev. Pharmacy* 1 (1), 24.
- Sharma, A.D., Underjeet, K., 2020. Molecular docking and pharmacokinetic screening of eucalyptol (1, 8 cineole) from eucalyptus essential oil against SARS-CoV-2. *Notulae Scientia Biologicae* 12 (3), 536–545.
- Sharma, A.D., 2020. Eucalyptol (1, 8 cineole) from eucalyptus essential oil a potential inhibitor of COVID 19 corona virus infection by molecular docking studies.
- Solans, C., Izquierdo, P., Nolla, J., Azemar, N., Garcia-Celma, M.J., 2005. Nano-emulsions. *Curr. Opin. Colloid Interface Sci.* 10 (3–4), 102–110.
- Song, J., Shi, F., Zhang, Z., Zhu, F., Xue, J., Tan, X., Zhang, L., Jia, X., 2011. Formulation and evaluation of celastrol-loaded liposomes. *Molecules* 16 (9), 7880–7892.

- Tulbah, A., 2021. COVID-19 Pandemic's Impact on Medication Dispensing and the use of Health Services in Makkah, Saudi Arabia. *J. Pharmaceut. Res. Int.*, 150–160.
- Tulbah, A.S., 2022. Inhaled Atorvastatin Nanoparticles for Lung Cancer. *Current Drug Delivery CDD* 19 (10), 1073–1082.
- Tulbah, A.S., Pisano, E., Scalia, S., Young, P.M., Traini, D., Ong, H.X., 2017. Inhaled simvastatin nanoparticles for inflammatory lung disease. *Nanomedicine* 12 (20), 2471–2485.
- Tulbah, A.S., Gamal, A., 2021. Design and Characterization of Atorvastatin Dry Powder Formulation as a potential Lung Cancer Treatment. *Saudi Pharmaceut. J.* 29 (12), 1449–1457.
- Tulbah, A.S., Lee, W.-H., 2021. Physicochemical Characteristics and In Vitro Toxicity/ Anti-SARS-CoV-2 Activity of Favipiravir Solid Lipid Nanoparticles (SLNs). *Pharmaceuticals* 14 (10), 1059.
- Tulbah, A.S., Ong, H.X., Colombo, P., Young, P.M., Traini, D., 2014. Novel simvastatin inhalation formulation and characterisation. *AAPS PharmSciTech* 15 (4), 956–962.
- Tulbah, A.S., Ong, H.X., Morgan, L., Colombo, P., Young, P.M., Traini, D., 2015. Dry powder formulation of simvastatin. *Expert Opin. Drug Deliv.* 12 (6), 857–868.
- Tulbah, A.S., Pisano, E., Landh, E., Scalia, S., Young, P.M., Traini, D., Ong, H.X., 2019. Simvastatin nanoparticles reduce inflammation in LPS-stimulated alveolar macrophages. *J. Pharm. Sci.* 108 (12), 3890–3897. <https://doi.org/10.1016/j.xphs.2019.08.029>.
- Valussi, M., Antonelli, M., Donelli, D., Firenzuoli, F., 2021. Appropriate use of essential oils and their components in the management of upper respiratory tract symptoms in patients with COVID-19. *J. Herbal Med.* 28, 100451.
- Wurtz, N., Penant, G., Jardot, P., Duclos, N., La Scola, B., 2021. Culture of SARS-CoV-2 in a panel of laboratory cell lines, permissivity, and differences in growth profile. *Eur. J. Clin. Microbiol. Infect. Dis.* 40 (3), 477–484.
- Yadalam, P.K., Varatharajan, K., Rajapandian, K., Chopra, P., Arumuganainar, D., Nagarathnam, T., Madhavan, T., 2021. Antiviral essential oil components against SARS-CoV-2 in pre-procedural mouth rinses for dental settings during COVID-19: A computational study. *Front. Chem.* 9, 86.
- Zhang, J., Zhan, B., Yao, X., Gao, Y., Shong, J., 1995. Antiviral activity of tannin from the pericarp of *Punica granatum* L. against genital Herpes virus in vitro. *Zhongguo Zhong yao za zhi= Zhongguo zhongyao zazhi= China journal of Chinese materia medica* 20 (9), 556–558. 576, inside backcover.